Int J Adv Manuf Technol (2010) 51:205–215
DOI 10.1007/s00170-010-2601-y

ORIGINAL ARTICLE

Prediction of surface characteristics obtained by burnishing

Afef Bougharriou · Wassila Bouzid Saï · Kacem Saï

Received: 24 December 2009 / Accepted: 24 February 2010 / Published online: 21 March 2010
© Springer-Verlag London Limited 2010

Abstract To reduce the irregularities of machined surface, burnishing is used as a finishing process by plastic deformation. This process does not only improve surface finish but also generates compressive residual stresses throughout the surface. In this work, an analytical study and a finite element modelling were performed to provide a fundamental understanding of the burnishing on an AISI 1042 workpiece. The analytical results were concentrated on the surface roughness and on some burnishing parameter effects. The simulations were devoted to the study of the surface profile, the residual stresses and the influence of burnishing parameters (penetration depth, feed rates, diameter of the ball of burnishing tool and initial surface quality) on surface roughness and the residual stress distribution. It has been noted that burnishing improves surface quality and introduces compressive residual stresses. These results were successfully compared to experimental data obtained in previous works.

Keywords Burnishing · Roughness · Residual stresses · Finite element modelling · Analytical modelling

1 Introduction

The machining process such as turning, milling, leaves irregularities on the surface, and it becomes necessary to carry out finishing operations in order to improve the state and the characteristics of the surface. Burnishing consists to the application of a pressure through a hard ball or roller. The tool generates a regular plastic deformation on the contact zone. Consequently, some modifications occur on the geometrical aspect of the surface, the residual stress level in the surface layer and some mechanical properties. To analyse the burnishing operation, an analytical model is established in this work to determine the obtained surface quality, to evaluate the parameters of roughness (the average roughness R_a and the total roughness R_t) and to study the influence of feed, penetration depth and ball diameter on the roughness evolution. A finite element (FE) model of the burnishing process was then built. The numerical results such as surface profile, residual stresses and the influence of burnishing parameters were evaluated and then compared with the experimental results obtained from the authors' previous works [1, 2].

Bouzid et al. [1] have established an analytical model to analyse the surface roughness after burnishing. This analytical model depends on the tool geometry, the initial surface roughness and the burnishing parameters (feed rate and penetration depth). The penetration depth of the burnishing tool is estimated by Hertz theory where the tool and the workpiece were supposed to have elastic behaviour. These authors have studied only the case for which the penetration depth is smaller than the initial surface roughness. In that study, the initial surface is obtained by turning or by grinding after turning. In the present study, the considered initial surface has a theoretical profile, which is generated by the cutting tool movement. The final surface profile depends also on the burnishing penetration depth, which can be smaller or higher than the initial total surface roughness. The burnishing penetration depth is estimated by the Hertz theory. Referring to this theory, the giving penetration depth is higher than the initial surface roughness. This case is presented in the present paper. It

A. Bougharriou (✉) · W. B. Saï · K. Saï
Unité de Génie de Production Mécanique et Matériaux, Ecole Nationale d'Ingénieurs de Sfax,
BP W 3038 Sfax, Tunisia
e-mail: afef.bougharriou@yahoo.fr

gives the lowest values of roughness comparing to the first case. Korzynski [3] has developed an analytical model, which includes the mechanical properties of the workpiece material, the geometry of the contact between workpiece and a spherical tool, the initial surface roughness and the penetration of the peaks of surface asperities. The developed model is restricted to a penetration less than the initial surface roughness. Black et al. [4] have estimated analytically the burnishing force, the depth of the final burnished layer and the plastic strain by using a slip-line model.

Bouzid et al. [2] have developed a three-dimensional (3D) FE model. The used model considers a cylindrical workpiece with an elastoplastic behaviour and a rigid ball. However, the initial surface is assumed to be perfect (smooth surface). The results were focused on the study of the material penetration, the residual stress distribution and the total roughness evolution with the feed. The total roughness qualifying the final surface is calculated by the mean of the analytical model determined in [1]. The residual stresses were analysed in a single point at the surface. Yen et al. [5] have also studied the burnishing process on an AISI 52100 workpiece by the mean of the FE method. They have established a 2D and a 3D model. The models consider a workpiece having an artificial surface roughness (regular surface profile) with an elastoplastic behaviour and a rigid ball. The simulation results, which are a comparison between the two models, are concentrated on the final surface profile and the residual stress distribution. The 3D model established in [5] has led to more realistic surface deformation compared to the 2D model. However, their 2D model seems to better predict the residual stresses than the 3D model.

Sartkulvanich et al. [6] have established a 2D model. In this model, the workpiece material is the same as the one used by Yen et al. [5]. The workpiece surface presents also an artificial roughness profile. The final surface profile, the residual stress distribution and the influence of feed rate and burnishing pressure on surface properties are predicted. Sartkulvanich et al. [6] have also studied the effect of initial residual stresses generated by hard turning. In the present study, the FE model considers a workpiece presenting a real surface roughness profile, which is obtained by turning. This real profile is taken into account in the mesh. The introduction of an artificial surface roughness would lead de facto, in the same way as the analytical model, to a final regular surface profile. From a qualitative point of view, the final surface will not look like a real experimental profile. Moreover, it is expected, with such approach to underestimate the roughness parameters.

The paper is organised in the following manner. In Section 2, the roughness parameters (R_a and R_t) are expressed with the burnishing parameters and the geometry of the burnishing tool. A study of the influence of the feed rate, the penetration depth and the diameter of the tool is given in that section. In Section 3, the FE modelling is explained in details. In that section, the geometric model and the used mesh are shown together with the boundary conditions and the material behaviour. Typical results, in terms of final surface roughness profile, residual stress distribution and a study of the influence of burnishing parameters (feed, penetration depth, speed, diameter of the tool and initial surface quality) on surface roughness and residual stresses are given. Section 4 is devoted to the comparison between the simulated and the experimental results. Some concluding remarks are given in the last section.

2 Analytical model

The workpiece is initially turned at 60 mm of diameter. The surface, which is generated by the turning tool, depends mainly on the feed rate f_T and the nozzle radius r_ε of the tool. Referring to the experimental data [1], the cutting parameters in turning are depth of cut p_T of 0.5 mm and feed f_T of 0.065 mm/tr. The carbide turning tool (P35) is characterised by a radius r_ε of 0.8 mm, an angle of attack ϕ of 5° and an angle of direction of the edge K_r of 95°. For the given turning parameters, the experimental profile has a total roughness R_{ti}, which is the maximum height between the higher peak and the lower valley along the evaluated length of 6.3 μm. The theoretical profile has an R_{ti} of 0.66 μm.

For a burnishing operation (Fig. 1) with an applied force F of 350 N [1], the penetration depth p_G (Eq. 1) of the burnishing tool is predicted by the Hertz theory. More details are given in the work of Bougharriou et al. [7].

$$p_G = \frac{310^{-3}\pi}{4a} r(K_1 + K_2)F \tag{1}$$

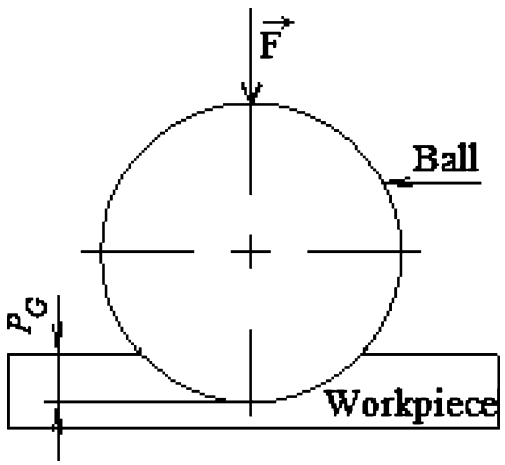

Fig. 1 Penetration depth of the burnishing operation

where K_1 and K_2 are, respectively, workpiece and tool material parameters. a denotes the semi axis, and r is a non-dimensional parameter. They are given by:

$$K_1 = \frac{1-\nu_1}{\pi E_1} \qquad K_2 = \frac{1-\nu_2}{\pi E_2} \tag{2}$$

$$a = m\left(\frac{3\pi(K_1+K_2)F}{2\left(C_1+C_1'+C_2+C_2'\right)}\right)^{\frac{1}{3}} \tag{3}$$

R_1, E_1 and ν_1 denote the radius, Young modulus and Poisson's ratio of the workpiece, respectively. R_2, E_2 and ν_2 denote the radius, Young modulus and Poisson's ratio of the burnishing ball, respectively.

C_1 and C'_1 are the maximum and the minimum curvature of the workpiece. C_2 and C'_2 are the maximum and the minimum curvature of the burnishing ball.

r and m depend on the angle φ [8], which is calculated as follows:

$$\cos\phi = \frac{R_2}{2R_1+R_2} \tag{4}$$

The penetration depth p_G estimated by the Hertz theory is 8.3 µm. The penetration depth p_G is higher than the initial roughness R_{ti} and the height of the asperities h_G.

$$\left(h_G = 125\frac{f_G^2}{R_2} = 0.12\,\mu\text{m},\ f_G = 0.065\ \text{mm/rev and}\ R_2 = 4.5\ \text{mm (radius of tool ball)}\right)$$

In this case, the final profile (Eq. 5) after burnishing is a series of intersection of circles arcs given by the positions i and $i+1$ of the ball (Fig. 2):

$$y(x) = \sqrt{4.5^2-(x-0.065i)^2} \quad \text{with} \quad i = E\left(\frac{x}{f_G}\right), \tag{5}$$

E is the integer part of $\left(\frac{x}{f_G}\right)$

The total roughness R_t, which is the maximum height between the higher peak and the lower valley along the evaluated length, is given by Eq. 6 and is equal to 0.11 µm (Fig. 3). The average roughness R_a of the final profile is given by Eq. 7. The parameter roughness R_a is determined by estimating a mean line x that divides equal areas beneath the surface profile between positive and negative regions [9] (Fig. 4). It is equal to 0.02 µm (Eq. 8).

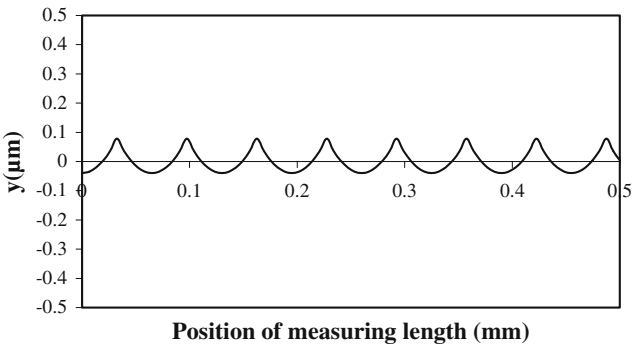

Fig. 2 Analytical burnished profile

$$R_t = h_G = R_2 - \sqrt{R_2^2 - \left(\frac{f_G}{2}\right)^2} \tag{6}$$

$$R_a = \frac{1}{n}\sum_{i=1}^{n} R_{ai} \text{ with } R_{ai} = \frac{1}{f_G}\int_{-\frac{f_G}{2}}^{\frac{f_G}{2}} |Y(x)|\mathrm{d}x \text{ and } n$$

$$= \frac{l}{f_G}\,(l \text{ is the base length}) \tag{7}$$

Y(x) is the equation of the profile defined to the mean line. $Y(x) = y(x) - y_{moy} = y(x) - \frac{1}{2}\left(R_2 + \sqrt{R_2^2 - \left(\frac{f_G}{2}\right)^2}\right)$, y_{moy} is the average value of $y(x)$. The average roughness R_a is then given by:

$$R_a = \left|\frac{R_2^2}{f_G}\,a\tan\frac{f_G}{2\sqrt{R_2^2-\left(\frac{f_G}{2}\right)^2}} - \frac{1}{2}R_2\right| \tag{8}$$

For the given penetration depth p_G, which is higher than the initial roughness R_{ti} and higher than the height of asperities h_G, which depends on feed, the analytical results (Fig. 5) show that the roughnesses R_a and R_t, which are modelled, respectively, by Eqs. 6 and 7, increase with the feed rate. After burnishing, the best surface quality is obtained for the feed of 0.065 mm/rev, which is the lowest feed.

The roughness parameters (Eqs. 6 to 7) are independent of the penetration depth. Note that in the case where the

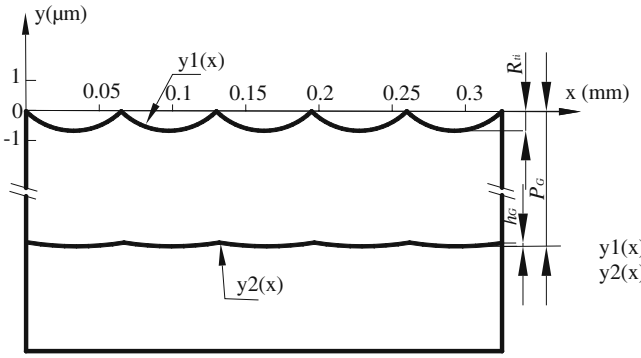

Fig. 3 Superposition of generated profiles obtained by cutting and burnishing tools

y1(x) profile generated with cutting tool
y2(x) profile generated with burnishing tool

penetration depth is lower than h_G, the equation of the profile (not discussed here due to the lack of space) is such as:

$$\begin{cases} y\,(x) = R_2 - p_G \quad \text{if} \quad x_{I_3} = f_G(i_2 - 1) + \sqrt{p_G(-p_G + 2R_2)} \le x \le x_{I_1} = i_2 f_G - \sqrt{p_G(-p_G + 2R_2)} \\ y(x) = \sqrt{R_2^2 - (x - i_2 f_G)^2} \quad \text{if} \quad x_{I_1} = i_2 f_G - \sqrt{p_G(-p_G + 2R_2)} \le x \le x_{I_2} = \sqrt{p_G(-p_G + 2R_2)} \\ i_2 = E\left(\dfrac{x}{f_G}\right) \end{cases} \tag{9}$$

This profile leads to expressions of the evolution of the total roughness R_t (R_t=p_G) and the average roughness R_a (Eq. 10). These expressions show that the roughness parameters R_t and R_a increase with the penetration depth of the burnishing tool.

$$R_a = \frac{1}{x_{I_3} - x_{I_2}} \left(\left| \left(\frac{p_G}{2}\right)(x_{I_1} - x_{I_3}) \right| + \left| \begin{array}{l} \dfrac{1}{2}(x_{I_2} - i_2 f_G)\sqrt{R_2^2 - (x_{I_2} - i_2 f_G)^2} + \dfrac{1}{2} R_2^2 a \tan \dfrac{x_{I_2} - i_2 f_G}{\sqrt{R_2^2 - (x_{I_2} - i_2 f_G)^2}} \\ - \dfrac{1}{2}(x_{I_1} - i_2 f_G)\sqrt{R_2^2 - (x_{I_1} - i_2 f_G)^2} - \dfrac{1}{2} R_2^2 a \tan \dfrac{x_{I_1} - i_2 f_G}{\sqrt{R_2^2 - (x_{I_1} - i_2 f_G)^2}} \\ - \left(R_2 - \dfrac{p_G}{2}\right)(x_{I_2} - x_{I_1}) \end{array} \right| \right) \tag{10}$$

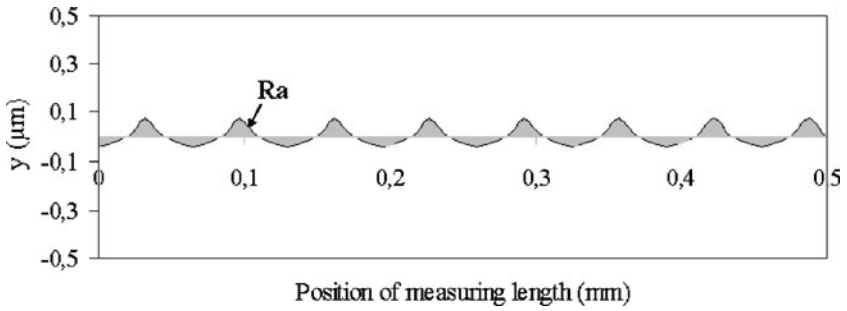

Fig. 4 The average roughness R_a

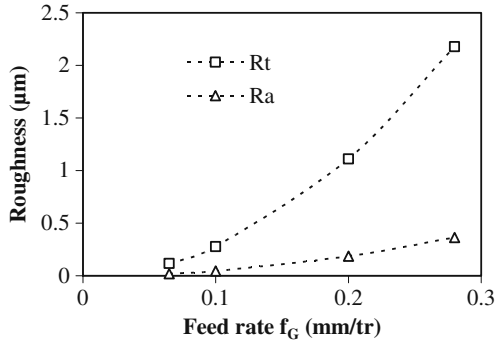

Fig. 5 Roughnesses evolution with feed for $p_G > R_{ti}$ and $p_G > h_G$

Figure 6 shows the evolution of roughness parameters with the diameter of the ball of the burnishing tool. For a feed of 0.065 mm/rev and a penetration depth of 8.6 µm higher than the height h_G, the results show that these roughness parameters decrease with the diameter of the tool.

3 Finite element modelling

The studied analytical model considers a workpiece with elastic behaviour instead of the realistic elastoplastic behaviour. The material behaviour may affect in a considerable way the obtained results. For that purpose, a FE model of the burnishing process is investigated in this section, taking into account the elastoplastic behaviour of the workpiece and the tool rigidity.

3.1 FE model description

The simulations were performed using the FE software Zebulon [10]. The modelling of the burnishing process concerns a cylindrical workpiece (Fig. 7). The workpiece diameter and length are, respectively, set to 30 and 4 mm. The initial workpiece surface is obtained by turning. The experimental roughness profiles are taken into account in the initial mesh (Fig. 7) (real surface profile). The mesh is computed by the linear interpolation of the measured data points. These points belong to the roughness surface and are sufficiently close to each other to correctly capture the surface irregularities (i.e. peaks and valleys). Each pair of neighbour point is the start and the end points of a straight line segment. The burnishing process is restricted to the simulation of a single pass of a rigid ball. The ball diameter of the burnishing tool is set to 9 mm. Because of the symmetries of the problem, the FE modelling considers only the eighth of the burnishing ball (tool) and the fourth of the cylindrical workpiece. The burnishing ball mesh includes 1,470 eight and six node elements. However, the workpiece is modelled with 11,025 eight and six node elements. Because of the extremely large computational time required for the simulation of the three-dimensional model, a simplified plane strain two-dimensional model is considered (Fig. 7). Some preliminary comparisons between the 2D and the 3D models are conducted to check the 2D model validity. Indeed, the results related to the 3D FE model show that the strain in the third axes is very small comparing with those in x and y directions. In this case, the burnishing ball was modelled with 261 four node elements. The workpiece mesh is generated using the software GMSH [11]. This tool guarantees a free mesh refined in the critical part of the surface in contact with the ball. The workpiece mesh includes 9,824 three node elements.

The contact between the tool and the workpiece is modelled by the classical Coulomb law with a friction parameter μ=0.1. The burnishing conditions are the feed rate of the tool set to f_G=0.065 mm/rev [1], the speed fixed to V=105 m/min [1] and the penetration depth of the tool evaluated to p_G=7.6 µm. The penetration depth p_G, corresponding to the experiment burnishing force of 350 N [1], is predicted from a 3D indentation simulation test.

The applied boundary conditions on the workpiece are shown in Fig. 7. To avoid sliding while in contact with the workpiece, the ball (tool) is subjected to a specific combination of the following movements:

- displacement along the y direction corresponding to the penetration depth of the tool ($Uy=p_G$)
- displacement along the x direction corresponding to the feed rate of the tool ($Ux=f_G$)

The coordinates of the point M (Fig. 8) at any time t is then given by:

$$x_M(t) = \rho\cos(\alpha+\theta(t)) - \rho\cos(\alpha) + \Delta x_c(t) \tag{11}$$

$$y_M(t) = \rho\sin(\alpha+\theta(t)) - \rho\sin(\alpha) + \Delta y_c(t) \tag{12}$$

$$\Delta x_c(t) = V_f t = \frac{60}{2\pi}\,\dot{\theta}\, f_G\, t = -R_2\theta(t) \tag{13}$$

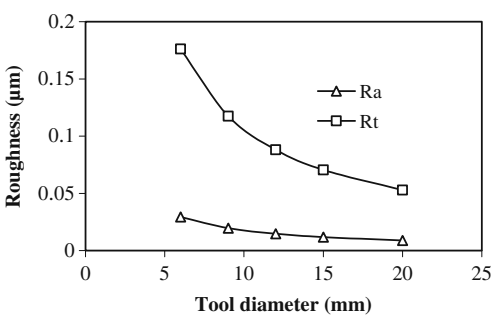

Fig. 6 Roughnesses evolution with tool diameter for $p_G > h_G$

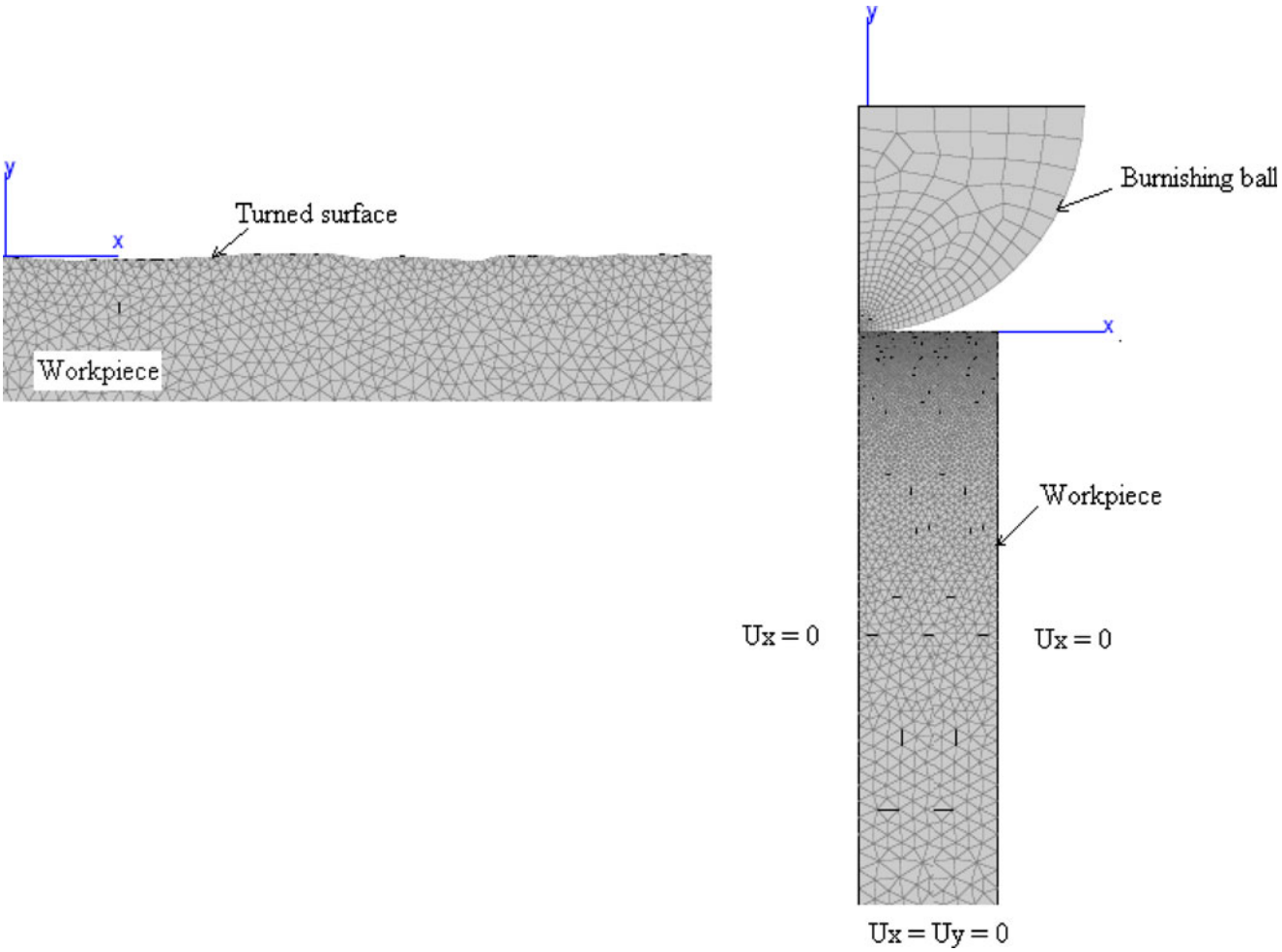

Fig. 7 Finite element mesh and boundary conditions

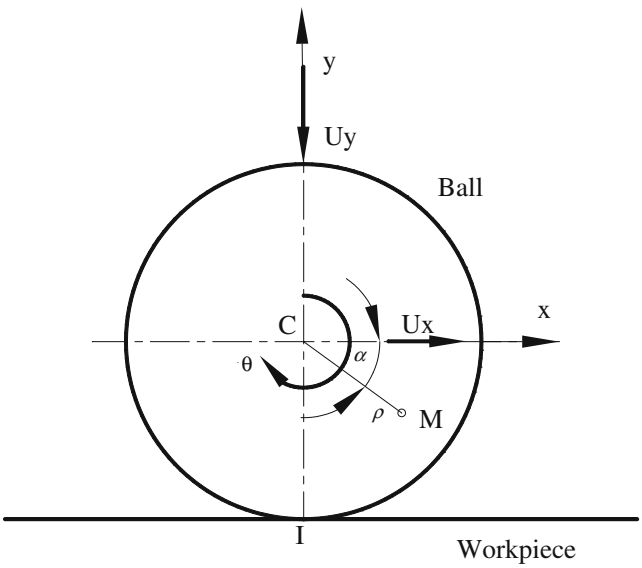

Fig. 8 Ball movements

where $\Delta x_c(t)$ and $\Delta y_c(t)$ are the displacements of the centre c along the x and the y directions, respectively:

$$\Delta y_c(t) = p_G \tag{14}$$

with $\dot{\theta} = \frac{2\pi n R_1}{6.10^4 R_2} = \frac{2\pi^2 V R_1^2}{3.10^7 R_2}$ given by the condition of rolling without sliding α and θ are, respectively, the angular position of the point M to the x axis and the speed angle of the ball. R_1 and R_2 are, respectively, the radius of the workpiece and the ball. ρ is the position of the point M far from the centre c.

The workpiece is assumed to have an elastoplastic behaviour. The total strain tensor is split into an elastic part and a plastic part. The elastic strain is given by the Hooke law.

$$\tilde{\varepsilon} = \tilde{\varepsilon}_e + \tilde{\varepsilon}_p \qquad \tilde{\sigma} = \tilde{\tilde{\Lambda}} : \tilde{\varepsilon}_e \tag{15}$$

The used unified model [12, 13] involves an isotropic hardening variable with non-linear expansion or contraction of a von Mises yield. Because of the lack of experimental

tests related to the material behaviour, kinematic hardening is not taken into account. The following von Mises yield function is used to describe the elastic domain.

$$f = J_2\left(\tilde{\sigma}\right) - R \qquad R = R_0 + Q(1 - \exp(-bp)) \tag{16}$$

In the case of a monotonous tensile test, the plastic strain ε_p is equal to the cumulated plastic deformation p. $J_2(\tilde{\sigma})$ is the second invariant of the deviator of the stress tensor $\tilde{\sigma}$. The variable R indicates the isotropic part of the hardening (expansion of the elastic domain). R_0 denotes the initial yield, Q is the hardening saturation (positive or negative) and b is the rate of saturation. The Young's modulus E, the Poisson's ratio ν and the values of model parameters were obtained by the best fit to the experimental tensile stress–strain curve [2] (Table 1).

3.2 Simulation results

In this section, the surface roughness profile of the burnished surface is predicted, and the average roughness R_a and the total roughness R_t are determined. These parameters are calculated for a base length of 0.5 mm on the middle of burnished zone far from the edges. Indeed, in the two-dimensional FE simulation, the workpiece is submitted to zero displacement on the right and on the left. The axial and the tangential residual stresses are also analysed in this section. The distribution of theses stresses through the depth from the machined surface is taken along four points located in the middle of the burnished surface. Moreover, a study of the effects of burnishing parameters (penetration depth, feed and diameter of the tool) on surface roughness and on the level of the residual stresses is performed.

3.2.1 Surface profile

Figure 9 shows the superposition of the initial and the final simulated profiles. The FE simulation of burnishing process shows that the surface quality of the workpiece is improved. The material is moved by plastic deformation by filling the valleys and by decreasing the height of the peaks. The roughness parameters R_a and R_t for a surface obtained by turning are, respectively, 1.33 and 6.3 μm. After burnishing, the simulation results show a reduction on the level of these parameters. The obtained roughnesses are 0.32 μm for R_a and 2.6 μm for R_t.

Table 1 Workpiece material parameters

E (GPa)	ν	R_0 (MPa)	Q (MPa)	b
210	0.3	300	*570*	11

3.2.2 Residual stress

Figure 10 shows the evolution of axial and tangential residual stresses, obtained by simulation, through the depth of the workpiece and at four points P1, P2, P3 and P4 located along the x direction, respectively, at 4.76×10^{-2}, 23.8×10^{-2}, 34.1×10^{-2} and 42×10^{-2} mm. The axial stress follows the x direction, while the tangential stress is the stress in the z direction. The normal residual stress in the y direction is very small compared to the axial and the tangential residual stresses. The FE results show that the burnishing process is at the origin of the compressive residual stresses in the surface layer of the workpiece. These stresses concern a depth almost of 600 μm. The axial and tangential residual stresses have the same variation. The numerical results show that the maximum values of these compressive residual stresses are located on the surface. These stresses (in terms of absolute values) decrease towards a depth of 600 μm from the machined surface. By increasing the depth, they increase and then decrease with change of sign and become negligible.

3.2.3 Effect of burnishing parameters

In this section, the results are focused on the effect of the burnishing parameter "penetration depth". The effect of the other parameters is then briefly described. For a feed of 0.065 mm/rev and a speed of 105 m/min, the simulation results (Fig. 11a) show that the average roughness R_a and the total roughness R_t decrease with the increase of the penetration depth up to an optimal value and then increase. In this case, the penetration depth giving the minimal values of roughnesses is about 7 μm. This result is explained by the fact that the increase of the penetration depth involves a rise of the burnishing force. As a consequence, the applied stress and then the action of the plastic deformation increase, which reduces the irregularities of the surface and the values of the roughnesses R_a and R_t until a certain limit. At this limit, the material is more deformed. Because of the imposed boundary conditions on the workpiece edges, the material is then escaped upwards when increasing the penetration depth. This leads to an increase of the level of the roughness parameters.

In terms of residual stresses, the simulation results (Fig. 11b) show that the average of the axial and the tangential residual stresses are influenced by the penetration depth of the burnishing tool. The value of the compressive residual stresses increases with the penetration depth. It is also noted that the affected depth grows also with the penetration depth. These results can be explained by the fact that by increasing the penetration depth, the burnishing force or pressure increases, which lead to the increase in the plastic deformation and

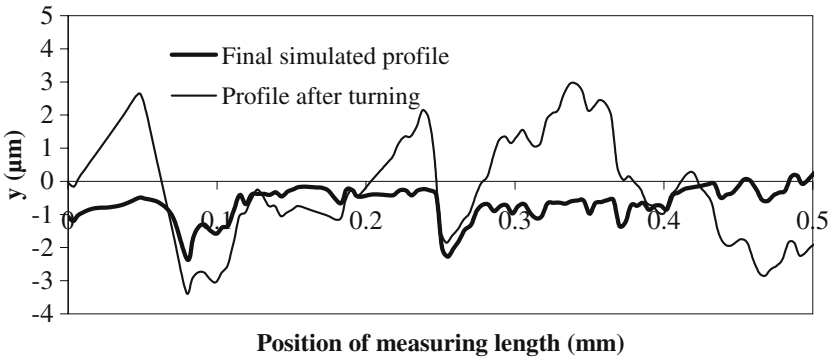

Fig. 9 Superposition of roughness profiles: profile after turning for p_T=0.5 mm, f_T=0.065 mm/rev and Vc=200 m/min; final simulated profile for p_G=7.6 µm, f_G=0.065 mm/rev and V=105 m/min

consequently to the increase of the compressive residual stresses and the affected depth.

The simulation results show that the increase of the feed involves the increase in the roughness parameters R_a and R_t. These results show also that the best surface quality is obtained for the lowest feed rate. In term of residual stresses, the simulation results show that the axial and the tangential residual stresses are weak influenced by the feed. The FE results show that the roughness parameters decrease first with the increase of the diameter of the tool and then increase slightly and finally stabilise.

4 Discussion

The experimental techniques used by Bouzid et al. [1] are first recalled. The burnishing process is carried out on a cylindrical workpiece with a diameter of 60 mm and a length of 20 mm obtained by turning, by a carbide tool. As for the burnishing tests, the used tool made of carbon chromium steel is a ball of 9 mm of diameter. The tool applies a force of 350 N on the machined surface. The friction and temperature elevation between tool and workpiece was limited by lubrication with oil. The surface profile was analysed in the feed direction using a DIAVITE roughness control instrument. The residual stresses were evaluated in terms of variation with the depth from machined surface by the X-ray diffraction method.

4.1 Surface profile

The surface quality is improved by burnishing. Under the action of the tool, the material is moved by plastic deformation by filling the valleys and decreasing the height of the peaks. Indeed, in the case of the AISI 1042 initially obtained by turning (Fig. 9), the analytical model (Fig. 2) and the FE modelling (Fig. 12b) of the burnished surface profile show as the experiment (Fig. 12a) that the final surface quality is improved. The surface profiles obtained by the two types of modelling differ from the experimental profile, leading to a difference in roughness values. The analytical model gives the lowest values. This result can be explained by the fact that the material spring back, and the position errors of the centre of the burnishing tool are not taken into account. The 2D FE model cannot predict exactly the values of the roughness parameters due to the numerical errors in the simulation, the

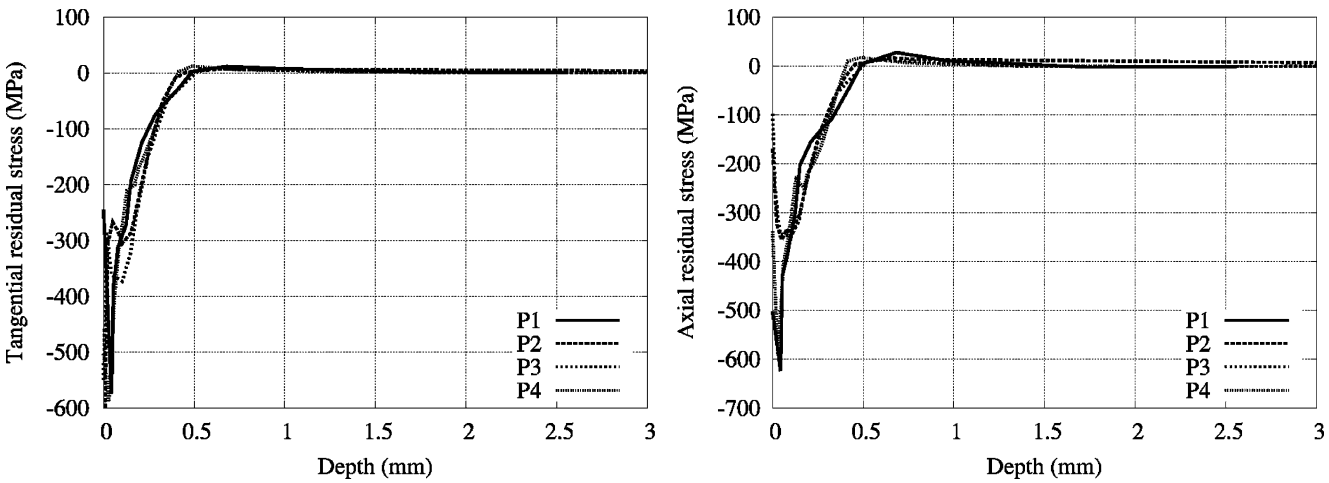

Fig. 10 FE results of axial and tangential residual stresses distributions through the depth obtained for p_G=7.6 µm, f_G=0.065 mm/rev and V=105 m/min

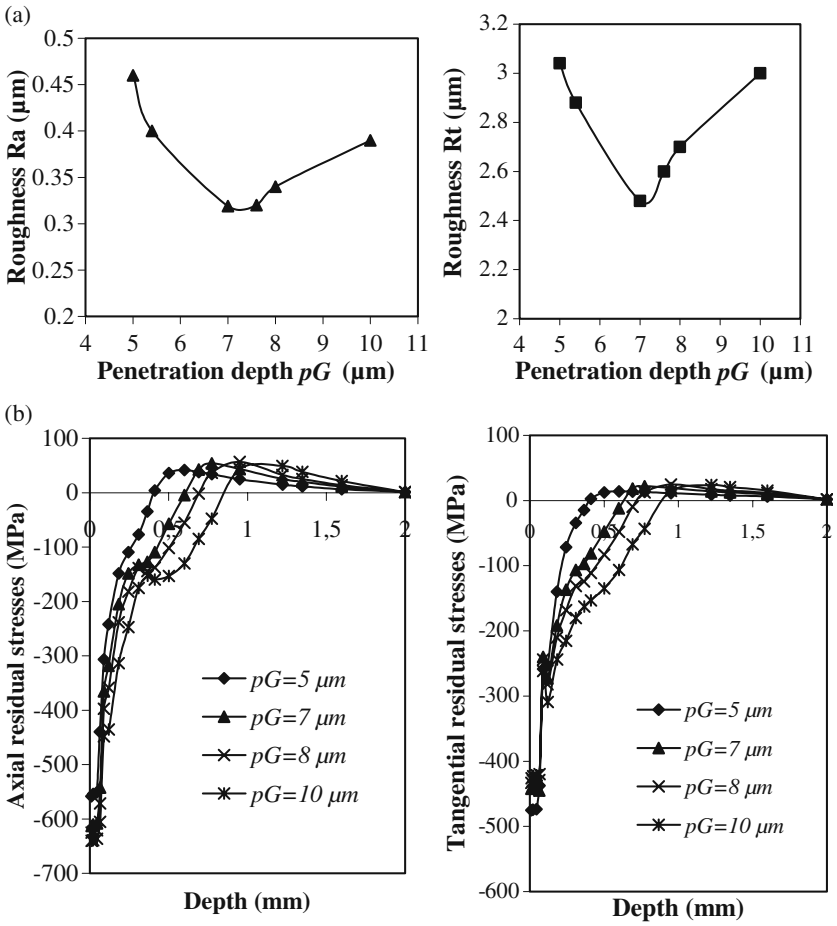

Fig. 11 Effect of penetration depth on **a** roughness evolution and **b** residual stresses evolution (f_G=0.065 mm/rev and V=105 m/min)

measurement errors from experiment, the consideration of a simplified plane strain model and the discrepancy in the working conditions. In the FE modelling, the workpiece is supposed to be fixed, which is not the case in the experiment.

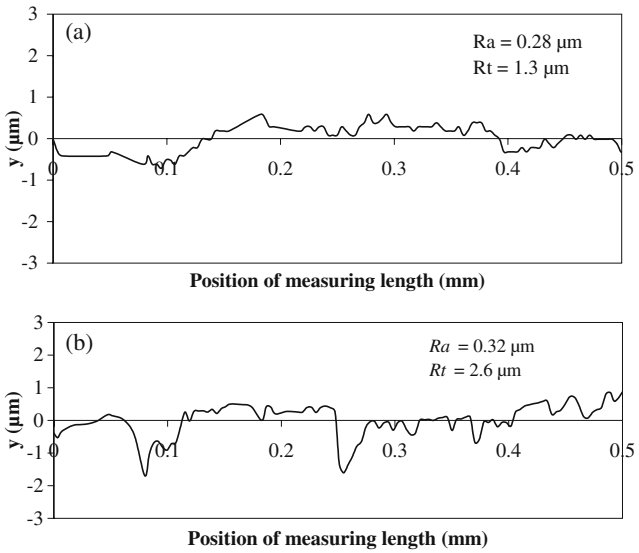

Fig. 12 Final profiles of AISI 1042 initially turned. **a** Experimental result, **b** FE result

According to the study of the two initial surface qualities (surface obtained by turning (*T*) and surface obtained by grinding after turning (*G*)), it can be noted that the surface quality after burnishing is linked to the initial surface. The initial surface obtained by grinding after turning led to a surface quality after burnishing (GB) better than that obtained by burnishing after turning (TB) (Fig. 13).

4.2 Residual stress

The FE analysis shows that the burnishing process produces compressive residual stress on the surface. The FE results are in agreement with the previous experiment [1]. Figure 14 gives the evolution of the axial and tangential residual stresses obtained by simulation and by experiment in the cases of the surface initially turned. The simulated axial residual stresses present the same evolution as the experiment. The introduced maximum residual stress by burnishing on the surface coincides with the experiment. Moreover, the 2D simulation with the plane strain hypothesis cannot provide the values of the tangential residual stresses. The average tangential residual stress value on the burnished surface is almost of −440 MPa, which is less (in terms of absolute value) than the experimental value

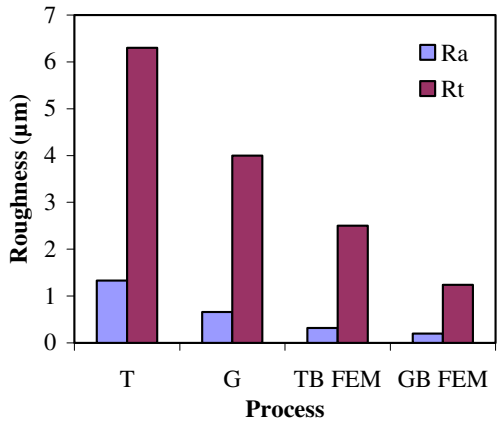

Fig. 13 Influence of the initial surface quality

(−962 MPa). In this case, a discrepancy is noted between the simulated and the experimental results. These differences are initially due to the initial residual stresses. The emission of heat during the formation of chip in turning process induces residual stresses on the machined surface of the workpiece. Before burnishing, the workpiece displays residual stresses caused by the turning process. Turning generates a traction axial residual stress and a compression tangential residual stress [1]. On the other hand, in the FE model, these initial residual stresses are not taken into account because of the absence of the initial and experimental field distribution of the residual stresses in the workpiece. Moreover, the axial and tangential residual stresses evolutions obtained by FE modelling fit well with the evolution of the average of stresses taken along the four points located in the middle of the burnished zone. However, the experimental results correspond to the evolution of the residual stresses along one point only.

4.3 Effect of penetration depth

The mean roughness and the total roughness decrease with the increase of the penetration depth up to an optimal value and then increase. Qualitatively, the FE modelling results are in agreement with the experimental results of Loh et al. [14].

The compressive residual stresses values increase with the penetration depth. It is also noted that the depth, starting from the surface and affected by the compressive residual stresses, increases with the penetration depth of the tool. These results are qualitatively in agreement with the results of Sartkulvanich et al. [6]. By increasing the penetration depth, the burnishing force or pressure increases, which leads to the increase of the residual stresses values.

5 Conclusion

In this study, an analytical model is carried out to characterise the final surface profile with geometrical and burnishing parameters. A 2D FE model is also carried out to predict the surface characteristics obtained by burnishing. The originality lies in the fact that the final surface quality is predicted using an initial surface having a real roughness profile, which is obtained by turning. The FE results are in agreement with the experiments. The obtained results show that the burnishing process improves surface quality. It gives a decrease of about 75% and 59%, respectively, for the average and the total roughness of the surface profile. The obtained results show also that the burnishing process generates a compressive residual stresses in the surface layer, and the affected depth depends essentially on the burnishing penetration depth. That may introduce an improvement of the mechanical characteristics of the surface. A simulation of the influence of some burnishing parameters is also carried out in order to predict the optimal values leading to a better quality of a machined surface. The obtained results lead to the following conclusions:

– The final surface depends on the burnishing tool penetration depth. For the studied model, a burnishing depth of 7 µm gives the reduced roughness parameters.

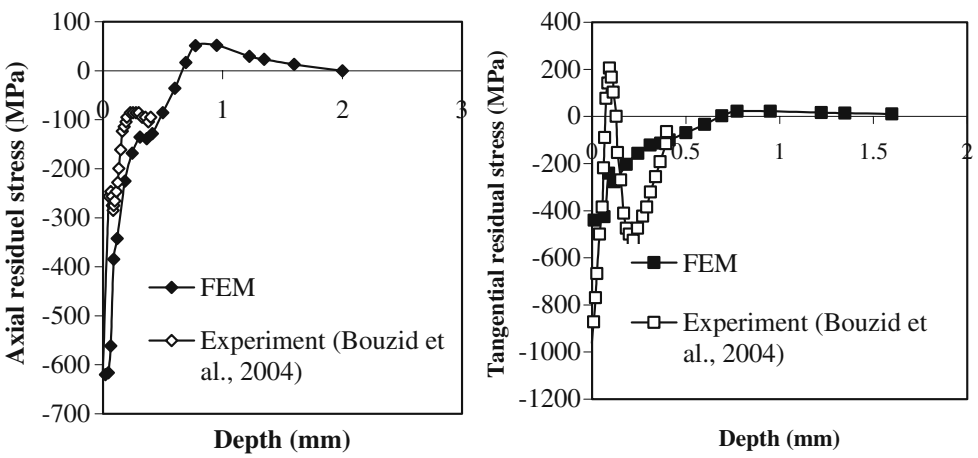

Fig. 14 Residual stresses distributions

- The best surface quality is obtained for the lowest feed.
- A burnishing tool diameter of 9 mm deals to the lowest values of roughnesses.
- The burnishing penetration depth presents a great influence on the residual stress and on the affected depth (depth which is affected by the compressive residual stress), whereas the feed rate introduces a weak effect.

The 2D FE model cannot predict precisely the values of the roughness parameters and residual stresses. To improve the results, the following points will be considered:

- The real workpiece material behaviour should be improved by the incorporation of a largest data base of experimental tests to fit the material parameters. In particular, special attention should be paid to the kinematic hardening.
- The use of the 3D FE model is conditioned by the availability of an experimental 3D roughness profile after turning.
- The initial residual stresses generated by the turning or grinding experimental processes should be taken into account in the FE modelling.

References

1. Bouzid W, Tsoumarev O, Saï K (2004) An investigation of surface roughness of burnished AISI 1042 steel. Int J Adv Manuf Technol 24:120–125
2. Bouzid W, Saï K (2005) Finite element modelling of burnishing of AISI 1042 steel. Int J Adv Manifact Technol 25:460–465
3. Korzynski M (2007) Modeling and experimental validation of the force surface roughness relation for smoothing burnishing with a spherical tool. Int J Mach Tools Manuf 47:1956–1964
4. Black AJ, Kopalinsky EM, Oxley PLB (1997) Analysis and experimental investigation of a simplified burnishing process. Int J Mech Sci 39:629–641
5. Yen YC, Sartkulvanich P, Altan T (2005) Finite element modelling of roller burnishing process. Engineering Research Center for Net Shape Manufacturing 54:237–240
6. Sartkulvanich P, Altan T, Jasso F, Rodriguez C (2007) Finite element modelling of hard roller burnishing: an analysis on the effects of process parameters upon surface finish and residual stress. J Manufact Sci Eng 129:705–716
7. Bougharriou A, Saï K, Bouzid W (2009) Finite element modelling of burnishing process. Mater Technol. doi:10.1179/175355509X387110
8. Johnson KL (1985) Contact mechanics. Cambridge University Press, Cambridge
9. Zani ML (2003) Mesures mécaniques: La mesure de rugosité Quelques normes et plusieurs dizaines de paramètres. Mesures 758:59–63
10. Besson J, Leriche R, Foerch R, Cailletaud G (1998) Object oriented programming applied to the finite element method. Part II. Application to material behaviours. Rev Eur Eléments finis 7:567–588
11. Geuzaine C, Remacle JF (1997–2009) An automatic 3D finite element mesh generator with built in pre- and post-processing facilities.
12. Chaboche JL (1977) Viscoplastic constitutive equations for the description of cyclic and anisotropic behavior of metals. Bull Pol Acad Pol Sci 25:33–48
13. Chaboche JL (1994) Cyclic viscoplastic constitutive equations Part I and II. ASME J Appl Mech 13:501–518
14. Loh NH, Tam SC, Miyazawat S (1990) Use of response surface methodology to optimize the finish in ball burnishing. Precis Eng 12:101–105